Dynamic CT-MPI + coronary CT angiography protocol

Calcium score was calculated to assess the calcification burden of each coronary branch. The scan range of dynamic stress CT-MPI was confirmed on the basis of the images of calcium score, covering the whole left ventricle and all epicardial vessels. Before the triggering of dynamic stress CT-MPI acquisition, adenosine triphosphate was intravenously infused at the rate of 160 μg/kg/min for 3 minutes. All subjects were injected with a fixed volume of contrast media (50 mL, Ultravist, 370 mg iodine/mL, Bayer) at the rate of 6 mL/s, followed by a 40 mL saline flush by using dual-barrel power injector (Tyco, Cincinnati, US). Dynamic stress CT-MPI acquisition was initiated 4 s after the beginning of contrast injection with a coverage of 10.5 cm for complete imaging of the whole left ventricle, using a shuttle mode technique. Image acquisition was triggered at the end-systolic phase (250 ms after the R wave). Scanning intervals depended on the participant's heart rate and scans were initiated every second or third heart cycle. Data acquisition was performed for 32 s with a total of 10 to 15 phases. The scan parameters of dynamic stress CT-MPI is listed as follow: gantry rotation time =250 ms, collimation =96×0.6 mm, automated tube current modulation (CARE Dose 4D, Siemens Healthineers) was used and the effective current =300 mAs, automated tube voltage modulation (CAREKv, Siemens Healthineers) was used and the reference tube voltage =80 kVp, reconstructed slice thickness =3 mm and reconstructed slice interval =2 mm.

All patients were given nitroglycerin 5 minutes after dynamic stress CT-MPI acquisition, prior to the acquisition of coronary CT angiography. A bolus tracking technique was used in CCTA acquisition and regions of interest was placed in the ascending aorta. A bolus of contrast media was intravenously injected at the rate of 4–5 mL/s, followed by injection of a 40 ml saline flush by using dual-barrel power injector. The dose of the contrast media was determined based on the patient's body weight (patients with body mass index <18 injected with 40 mL contrast media at 4 mL/s, patients with body mass index between 18 and 24 injected with 50 mL contrast media at 4.5 mL/s, patients with body mass index >24 injected with 60 mL contrast media at 5 mL/s). CCTA images were obtained by using prospective ECG-triggered sequential acquisition, with the acquisition window covering from 35% to 75% of R-R interval, with gantry rotation time =250 ms collimation =96×0.6 mm, reconstructed slice thickness =0.75 mm, reconstructed slice interval =0.5 mm and application of CAREKv and CARE Dose 4D. The reference tube current was set as 320 mAs and the reference tube voltage was set as 100 kVp.

Plaque analysis and CT-FFR simulation

CCTA datasets were reconstructed with smooth kernel (Bv 40) and third generation iterative reconstruction (IR) technique (strength 3, ADMIRE, Siemens). A dedicated research software (Coronary Plaque Analysis, version 4.3, Siemens Healthineers, Germany) was employed for further analysis of all lesions with stenosis extent ≥30% at any epicardial vessel with diameter ≥2 mm. The following indices were measured and recorded: (I) diameter stenosis (DS) was calculated as (reference diameter – minimal lumen diameter)/reference diameter and was measured manually with a digital caliper at the narrowest level of the lesion and the proximal reference on the cross-sectional images; (II) remodeling index was defined as a maximal lesion vessel diameter divided by proximal reference vessel diameter (at the site where no plaque component can be detected), with positive remodeling (PR) defined as a remodeling index ≥1.1; (III) low-attenuation plaque (LAP) was defined as non-calcified plaques with low-density components (CT value <30 HU); (IV) spotty calcification (SC) was defined by an intra-lesion calcific plaque <3 mm in length that comprised <90 degrees of the lesion circumference; (V) Napkin-ring sign (NRS) was characterized by a plaque core with low attenuation areas on CT surrounded by a rim-like area of higher attenuation (CT value ≤130 HU) as previously reported. HRPs were defined as plaques with at least two HRP (LAP, PR, NRS and SC) features. The coronary stenosis of individuals was evaluated according to Coronary Artery Disease - Reporting and Data System (CAD-RADS) and patients with CAD-RADS grade 3 or above were considered the presence of obstructive CAD.

Lesion-specific CT-FFR values were measured for all stenosis with DS ≥30% at any epicardial vessel with diameter ≥2 mm. The current study used a machine learning (ML)-based approach, which is an alternative to physics-based approach and can be used on-site to simulate CT-FFR (cFFR, version 3.0, Siemens Healthineers, Forchheim, Germany). It's trained using a synthetically generated database of 12,000 different anatomies of coronary arteries with randomly placed stenosis among

https://dx.doi.org/10.21037/cdt-21-219

different branches and bifurcations. A computational fluid dynamic (CFD) by solving reduced-ordered Navier-Stokes equations is applied to calculate the pressure and flow distribution for each coronary tree. Quantitative features of anatomy and computed CT-FFR value were extracted for each location along the coronary tree. Then deep machine learning model is trained by using a deep neural network with four hidden layers to learn the relationship between the FFR value and quantitative anatomic features.

For the on-site processing, the centerline and luminal contours for whole coronary tree were automatically generated after CCTA data were successfully loaded. The centerline and luminal contour which can be manually adjusted when needed are fundamental and critical information for computing CT-FFR value. Users need to label all stenotic lesions manually to extract their geometrical features required for cFFR algorithm. Finally, those data were input into the pre-learned model and cFFR at all locations were generated automatically, and the resulting values were visualized by color-coded 3D coronary maps. The lesion-specific CT-FFR values were measured at the distal shoulder of the lesion, where no plaque could be detected.

Table S1 Intra-observer reproducibility

Variables	ICC	95% CI	P value
DS (%)	0.907	0.828–0.950	<0.001
$MBF_{ischemic}$	0.938	0.887–0.967	<0.001
MBF_{ratio}	0.939	0.888–0.967	<0.001
CT-FFR	0.921	0.840–0.960	<0.001
Spotty calcium	0.884	0.827–0.923	<0.001
Napkin-ring sign	0.877	0.818–0.918	<0.001
Positive remodeling	0.911	0.844–0.950	<0.001
Low attenuation plaque	0.893	0.831–0.933	<0.001

CI, confidence interval; ICC, intraclass correlation coefficient; DS, diameter stenosis; CT-FFR, computed tomography fractional flow reserve; MBF, myocardial blood flow.

Table S2 Inter-observer reproducibility

Variables	ICC	95% CI	P value
DS (%)	0.913	0.842–0.953	<0.001
$MBF_{ischemic}$	0.928	0.868–0.961	<0.001
MBF_{ratio}	0.922	0.857–0.958	<0.001
CT-FFR	0.911	0.826–0.954	<0.001
Spotty calcium	0.824	0.745–0.880	<0.001
Napkin-ring sign	0.840	0.767–0.891	<0.001
Positive remodeling	0.873	0.783–0.926	<0.001
Low attenuation plaque	0.857	0.782–0.908	<0.001

CI, confidence interval; ICC, intraclass correlation coefficient; DS, diameter stenosis; CT-FFR, computed tomography fractional flow reserve; MBF, myocardial blood flow.

https://dx.doi.org/10.21037/cdt-21-219

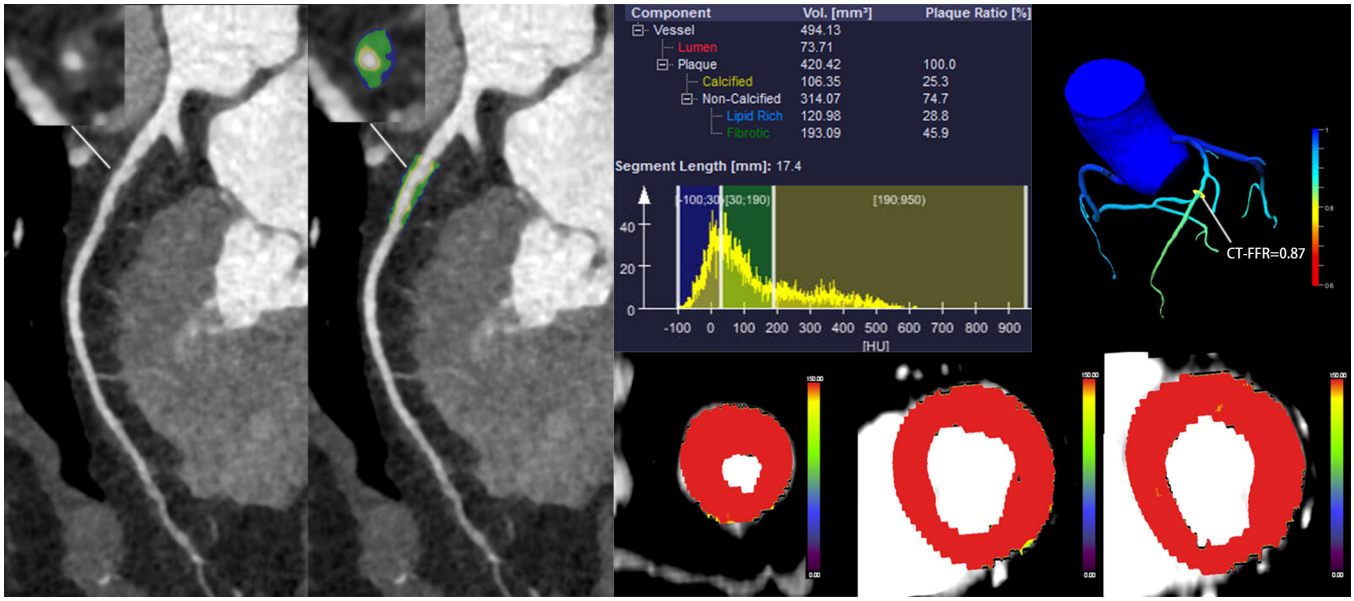

Figure S1 Representative case of patient without MACE. A 69-year-old female with atypical chest pain underwent CCTA + dynamic CT-MPI. CCTA showed mixed plaque with mild stenosis at proximal LAD. This lesion was revealed to have two HRP features (LAP and PR) and hemodynamically insignificant with CT-FFR value of 0.87. Dynamic CT-MPI demonstrated normal myocardial perfusion, with global MBF of 215 mL/100 mL/min. This patient was MACE free during a follow-up period of 17 months. CCTA, coronary computed tomography angiography; CT-FFR, computed tomography fractional flow reserve; CT-MPI, computed tomography myocardial perfusion imaging; LAD, left anterior descending; LAP, low attenuation plaque; MACE, major adverse cardiac event; MBF, myocardial blood flow; PR, positive remodeling.

https://dx.doi.org/10.21037/cdt-21-219